# Optimal Data Rate Allocation for Dynamic Sensor Fusion over Resource Constrained Communication Networks

Hyunho Jung<sup>1</sup>

Takashi Tanaka<sup>2</sup>

Abstract—We consider a dynamic sensor fusion problem where a large number of remote sensors observe a common Gauss-Markov process and the observations are transmitted to a fusion center over a resource constrained communication network. The design objective is to allocate an appropriate data rate to each sensor in such a way that the total data traffic to the fusion center is minimized, subject to a constraint on the fusion center's state estimation error covariance. We show that the problem can be formulated as a difference-of-convex program, to which we apply the convex-concave procedure (CCP) and the alternating direction method of multiplier (ADMM). Through a numerical study on a truss bridge sensing system, we observe that our algorithm tends to allocate zero data rate to unneeded sensors, implying that the proposed method is an effective heuristic for sensor selection.

# I. INTRODUCTION

The advancement of low-cost sensing technologies made a large amount of data easily accessible in control systems. While this is advantageous from the conventional controltheoretic viewpoints, engineers now face the issue of excessive data rate that often overwhelms systems' communication resources. Consequently, how to strategically discard superfluous sensor data is a relevant question to many applications.

In this paper, we consider a dynamic sensor fusion problem over a resource constrained communication network. Our primary focus is to optimize the allocation of scarce communication resources across a subset of different sensors. Our problem is closely related to several sensor selection problems that have been studied widely in the literature. In [1], the authors approaches the sensor selection problem to minimizes the determinant of the covariance matrix of estimation error via a semidefinite programming (SDP) relaxation. In [2], energy constrained wireless network was considered and solved using the re-weighted  $\ell_1$  relaxation. The reference [3] applied stochastic dynamic programming to gather adequate information for multi-stage problem for control of a robotic assembly task. A structure sensor placement problem was considered in [4], where an iterative technique involving the Fisher information matrix (FIM) was developed. The work [5] also considered determinant of FIM and used genetic algorithm, which selects subset of sensor positions maximizing the determinant of the matrix. Structure sensor placement problems were also considered

in [6] and [7]. In [8], mutual information (MI) was adopted as the information gain metric and was applied to a target location tracking problem using distributed sensors. The reference [9] introduced an approximation algorithm which estimates position of a target. The algorithm selects competitive sensors to guarantee estimation error within factor 2 of optimal choice under condition that the measurements are merged.

The problem considered in this paper is different in that we not only aim to select a subset of sensors, but also try to allocate an appropriate data rate to each sensor to minimize overall communication cost subject to a constraint on estimator accuracy. We first invoke basic results on entropy-coded data quantizers from the source coding literature to show that the communication data rate (measured in bits) from each sensor to the fusion center can be well-approximated by the MI between certain random variables. Based on this observation, we formulate an optimization problem (which is referred to as the sensor resource allocation (SRA) problem in the sequel) in which the sum of MI terms over all communication links is minimized subject to a constraint on the mean-square error (MSE) estimation performance achievable by the fusion center. Then, the SRA problem is formulated as a difference-of-convex program [10] to which we apply the heuristics of convex-concave procedure. Although our problem formulation is not combinatorial in nature, notably, the proposed mechanism is sparsity-promoting – the algorithm tends to identify unneeded sensors by allocating them zero data rates, and the number of unneeded sensors tends to increase as the constraint on the MSE performance is made less stringent. Therefore, the proposed method can be used as a new and effective heuristic for sensor selection.

This paper is organized as follows. In Section II, we formulate the SRA problem after reviewing the method of entropy-coded dithered-quantizers (ECDQ). In Section III, the SRA problem is reformulated as a difference-of-convex program. We propose practical solution approaches based on the CCP and the ADMM in Section IV. Numerical demonstrations on a truss bridge sensor placement problem are presented in Section V. We conclude in Section VI.

Notation: Lower case boldface symbols such as  $\mathbf{x}$  are used to denote random variables. We use  $\mathbf{x}_{1:t} = (\mathbf{x}_1,...,\mathbf{x}_t)$  to denote the random process. We adopt standard notation for information-theoretic functions [11]: the entropy of a discrete random variable  $\mathbf{x}$  is denoted by  $H(\mathbf{x})$ , while the differential entropy of a continuous random variable  $\mathbf{x}$  is denoted by  $h(\mathbf{x})$ . The mutual information between  $\mathbf{x}$  and  $\mathbf{y}$  is denoted by  $I(\mathbf{x};\mathbf{y})$ , and the relative entropy is denoted by  $D(\cdot||\cdot)$ .

<sup>\*</sup>This work is supported by DARPA Grant D19AP00078, FOA-AFRL-AFOSR-2019-0003 and NSF Award 1944318.

<sup>&</sup>lt;sup>1</sup>H. Jung is with the Department of Mechanical Engineering, University of Texas at Austin, TX 78712, USA. jung.hyunho@utexas.edu

<sup>&</sup>lt;sup>2</sup>T. Tanaka is with the Department of Aerospace Engineering and Engineering Mechanics, University of Texas at Austin, TX 78712, USA. ttanaka@utexas.edu

We use  $\mathbb{S}^n$  for the set of symmetric matrices of size  $n \times n$ . For  $X \in \mathbb{S}^n$ ,  $X \in \mathbb{S}^n_+$  or  $X \succeq 0$  means that X is a positive semidefinite matrix, and  $X \in \mathbb{S}^n_{++}$  or  $X \succ 0$  means that X is a positive definite matrix.

#### II. PROBLEM FORMULATION

We consider a remote estimation problem over a sensor network shown in Fig. 1. The random process to be estimated is a discrete-time, *n*-dimensional Gauss-Markov process

$$\mathbf{x}_{t+1} = A\mathbf{x}_t + F\mathbf{w}_t, \ \mathbf{w}_t \stackrel{i.i.d.}{\sim} \mathcal{N}(0, I), \ t = 1, 2, ..., T$$
 (1)

with  $\mathbf{x}_1 \sim \mathcal{N}(0, P_{1|1})$ , where matrices  $A \in \mathbb{R}^{n \times n}$  and  $P_{1|1} \in \mathbb{S}^n_+$  are given. There are M distributed sensors, each making a scalar-valued noiseless measurement  $\mathbf{y}_{i,t} = C_i \mathbf{x}_t$ , i = 1, 2, ..., M. For convenience, we write  $\mathbf{y}_t = C \mathbf{x}_t$  where

$$\mathbf{y}_t = \begin{bmatrix} \mathbf{y}_{1,t} \\ \vdots \\ \mathbf{y}_{M,t} \end{bmatrix}, \quad C = \begin{bmatrix} C_1 \\ \vdots \\ C_M \end{bmatrix} \in \mathbb{R}^{M \times n}.$$

Throughout the paper, the pair (A, C) is assumed to be observable.

#### A. Data fusion over resource-constrained network

We consider the situation in which the output  $y_{i,t}$  of remote sensors must be transmitted to the data fusion center over a resource-limited communication network. The network model we introduce in this section assumes a CANbus-like communication system. All the nodes in the network operate synchronously in discrete-time. At every time step t, each sensor i = 1, 2, ..., M encodes  $\mathbf{y}_{i,t}$  into a packet  $\mathbf{z}_{i,t}$ . For each i and t, we assume that  $\mathbf{z}_{i,t}$  is a uniquely decodable variable-length binary codeword with length  $\ell_{i,t}$ . Packets  $\mathbf{z}_{i,t}$  from sensors are received by the fusion center reliably (no packet losses, no bit flips) without delay. They are decoded by the fusion center where the least mean-square error (MSE) estimate  $\hat{\mathbf{x}}_{t|t}$  of the source process (1) is computed. Based on  $\hat{\mathbf{x}}_{t|t}$ , the fusion center also computes a step-ahead prediction  $\hat{\mathbf{x}}_{t+1|t} := A\hat{\mathbf{x}}_{t|t}$ . Once  $\hat{\mathbf{x}}_{t+1|t}$  is computed, we further assume that the fusion center broadcasts  $\hat{\mathbf{x}}_{t+1|t}$  back to all the sensors (Fig. 1), which allows each sensor to apply the predictive quantizer at time step t+1. We assume that the feedback channel delivers the  $\mathbb{R}^n$ -valued message  $\hat{\mathbf{x}}_{t+1|t}$ reliably.3

 $^3$ This assumption holds if the feedback message is given a sufficiently large codeword length so that the effect of quantization is negligible. Allowing feedback messages to have large blocklengths is a reasonable design since the backward channel delivers only one message per time step, whereas the forward channel delivers at most M messages per time step.

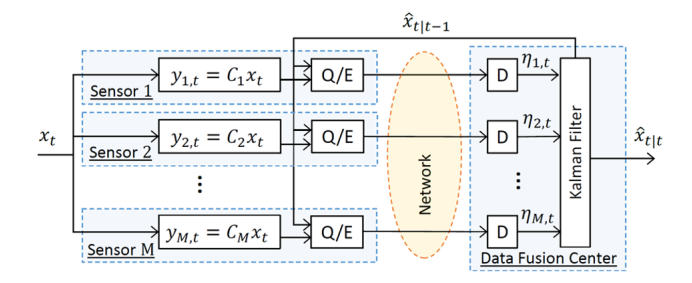


Fig. 1. Distributed sensors and data fusion center.

## B. Entropy-coded dithered quantizer (ECDQ)

At each sensor node i, the continuous random variable  $\mathbf{y}_{i,t}$  is first quantized into a discrete random variable, which is then encoded as a binary codeword  $\mathbf{z}_{i,t}$ . We assume that this process is implemented by the so-called *entropy-coded dithered quantizer (ECDQ)* mechanism [14] shown in Fig. 2(a). The ECDQ is easy to implement in practice, its mathematical analysis is relatively simple, and it attains a near-optimal performance (that is, the expected codeword length is close to the fundamental lower bound). As shown in Fig. 2(a), in time step t, the innovation signal  $\theta_{i,t} = \mathbf{y}_{i,t} - C_i \hat{\mathbf{x}}_{t|t-1}$  is first computed. It is then quantized by the dithered uniform quantizer with quantization step size  $\Delta_{i,t}$ :

$$\begin{split} Q_{\Delta_{i,t}}(\boldsymbol{\theta}_{i,t} + \boldsymbol{\xi}_{i,t}) &= k \Delta_{i,t} \\ &\text{if } (k - \frac{1}{2}) \Delta_{i,t} \leq \boldsymbol{\theta}_{i,t} + \boldsymbol{\xi}_{i,t} < (k + \frac{1}{2}) \Delta_{i,t}. \end{split}$$

Here,  $\xi_{i,t} \stackrel{i.i.d.}{\sim} \text{unif}[-\frac{\Delta_{i,t}}{2}, \frac{\Delta_{i,t}}{2}]$  is an artificial random variable called dither. The dither signal may not be necessary for practical implementations, but it simplifies the mathematical analysis of the communication system. The output  $\mathbf{q}_{i,t}$  is then encoded into a binary codeword  $\mathbf{z}_{i,t} \in \{0,1\}^{\ell_{i,t}}$  using an entropy-based data-compression scheme (e.g., Huffman code, Shannon-Fano code). Notice that the codeword length  $\ell_{i,t}$  is a random variable. The codeword  $\mathbf{z}_{i,t}$  is decoded losslessly as  $\mathbf{q}_{i,t} = D(\mathbf{z}_{i,t})$  by the data fusion center. Then the dither signal is subtracted to compute  $\eta_{i,t} = \mathbf{q}_{i,t} - \xi_{i,t}$ , which is used for the belief update in the Kalman filter as shown in Fig. 2(a). Notice that the end-to-end effect of the ECDQ with input  $\theta_{i,t}$  and output  $\eta_{i,t}$  is

$$\boldsymbol{\eta}_{i,t} = Q_{\Delta_{i,t}}(\boldsymbol{\theta}_{i,t} + \boldsymbol{\xi}_{i,t}) - \boldsymbol{\xi}_{i,t}. \tag{2}$$

It can be shown [15] that (2) is mathematically equivalent to

$$\boldsymbol{\eta}_{i,t} = \boldsymbol{\theta}_{i,t} + \mathbf{v}_{i,t}, \quad \mathbf{v}_{i,t} \stackrel{i.i.d.}{\sim} \operatorname{unif}\left[-\frac{\Delta_{i,t}}{2}, \frac{\Delta_{i,t}}{2}\right]$$
(3)

where the quantization noise  $\mathbf{v}_{i,t}$  is independent of  $\boldsymbol{\theta}_{i,1:t}$ . The equivalence between (2) and (3) means that the channel models in Fig. 2(a) and Fig. 2(b) are equivalent, which simplifies the performance analysis.

#### C. Approximation of communication cost

We call the expected codeword length  $R_i := \frac{1}{T} \sum_{t=1}^T \mathbb{E}(\ell_{i,t})$  the *rate* allocated to sensor i. The next lemma shows a relationship between the rate  $R_i$  and the mutual information  $I(\boldsymbol{\theta}_{i,t}; \boldsymbol{\eta}_{i,t})$ :

 $<sup>^1</sup>$ In reality, a packet frame in the CAN protocol contains a header and a tailer in addition to the data field. For simplicity, we assume  $\ell_{i,t}$  only represents the lengths of the data field, ignoring the header and footer bits.

<sup>&</sup>lt;sup>2</sup>To improve the coding efficiency, it is known to be more advantageous to quantize and encode the *innovation*  $\mathbf{y}_{i,t+1} - C\hat{\mathbf{x}}_{t+1|t}$  than  $\mathbf{y}_{i,t+1}$  itself. See, e.g., [12] [13].

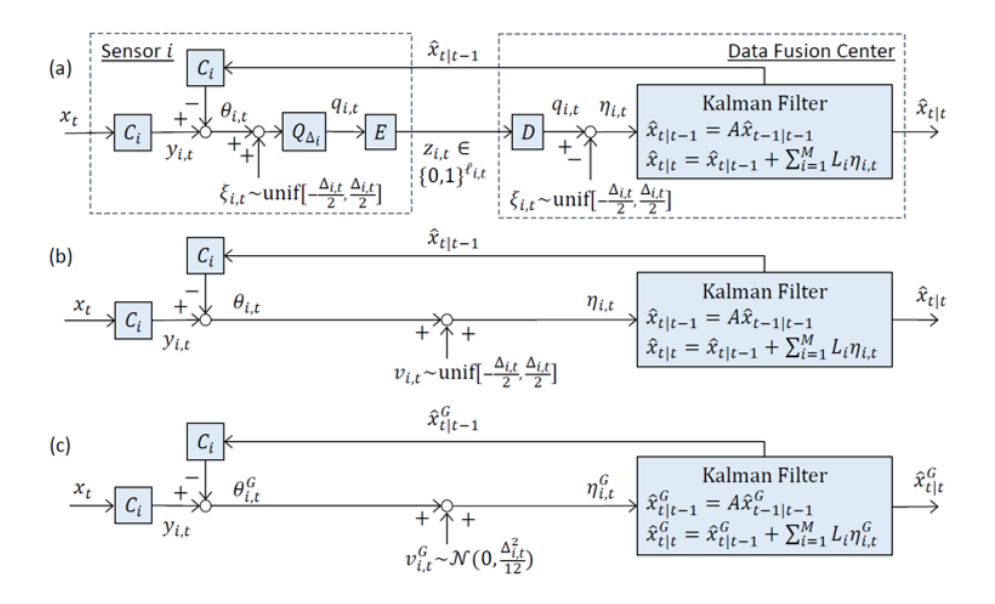


Fig. 2. (a) Channel model. (b) Equivalent channel model. (c) Simplified channel model.

**Lemma 1:** For every i and t, we have

$$I(\boldsymbol{\theta}_{i,t}; \boldsymbol{\eta}_{i,t}) \leq \mathbb{E}(\boldsymbol{\ell}_{i,t}) < I(\boldsymbol{\theta}_{i,t}; \boldsymbol{\eta}_{i,t}) + 1$$

where the mutual information is evaluated under the joint distribution defined by the diagram in Fig. 2(b).

*Proof:* Due to the page limitation, the proof is deferred to the extended version<sup>4</sup> of this paper.

Since  $\boldsymbol{\theta}_{i,t}$  and  $\boldsymbol{\eta}_{i,t}$  in Fig. 2(b) are not Gaussian random variables, it is difficult to evaluate  $I(\boldsymbol{\theta}_{i,t};\boldsymbol{\eta}_{i,t})$  directly. A common approach (e.g., [16]) is to evaluate  $I(\boldsymbol{\theta}_{i,t}^G;\boldsymbol{\eta}_{i,t}^G)$  instead, where  $\boldsymbol{\theta}_{i,t}^G$  and  $\boldsymbol{\eta}_{i,t}^G$  are Gaussian random variables defined by the diagram in Fig. 2(c). In Fig. 2(c), the quantization noise  $\mathbf{v}_{i,t} \overset{i.i.d.}{\sim} \text{unif}[-\frac{\Delta_{i,t}}{2},\frac{\Delta_{i,t}}{2}]$  is replaced by a Gaussian random variable  $\mathbf{v}_{i,t}^G \overset{i.i.d.}{\sim} \mathcal{N}(0,V_{i,t})$ , where we set  $V_{i,t} = \frac{\Delta_{i,t}^2}{12}$  so that  $\mathbf{v}_{i,t}$  and  $\mathbf{v}_{i,t}^G$  share the same covariance. Consequently,  $\{\mathbf{x}_{t|t}^G, \mathbf{x}_{t|t-1}^G, \boldsymbol{\theta}_t^G, \boldsymbol{\eta}_t^G\}_{t=1,2,\dots,T}$  are jointly Gaussian random variables with the same mean and covariance as  $\{\mathbf{x}_{t|t}, \mathbf{x}_{t|t-1}, \boldsymbol{\theta}_t, \boldsymbol{\eta}_t\}_{t=1,2,\dots,T}$ . The following lemma provides an estimate of  $I(\boldsymbol{\theta}_{i,t}^G; \boldsymbol{\eta}_{i,t}^G)$ :

# Lemma 2:

$$I(\boldsymbol{\theta}_{i,t}^{\text{G}}; \boldsymbol{\eta}_{i,t}^{\text{G}}) \leq I(\boldsymbol{\theta}_{i,t}; \boldsymbol{\eta}_{i,t}) < I(\boldsymbol{\theta}_{i,t}^{\text{G}}; \boldsymbol{\eta}_{i,t}^{\text{G}}) + \frac{1}{2}\log\frac{2\pi e}{12}.$$

Proof: Please refer to the extended version.

From Lemma 1 and Lemma 2, we obtain

$$I(\boldsymbol{\theta}_{i,t}^{\mathrm{G}}; \boldsymbol{\eta}_{i,t}^{\mathrm{G}}) \leq \mathbb{E}(\boldsymbol{\ell}_{i,t}) < I(\boldsymbol{\theta}_{i,t}^{\mathrm{G}}; \boldsymbol{\eta}_{i,t}^{\mathrm{G}}) + \underbrace{1 + \frac{1}{2} \log \frac{2\pi e}{12}}_{\approx 1.254 \mathrm{[bits]}}. \tag{4}$$

This inequality implies that evaluating  $I(\theta_{i,t}^G; \eta_{i,t}^G)$  under the diagram Fig. 2(c) gives an estimate of the rate of the ECDQ

under the architecture of Fig. 2(a) within the accuracy of 1.254 bits per time step. Notice that  $I(\boldsymbol{\theta}_{i,t}^{G}; \boldsymbol{\eta}_{i,t}^{G})$  depends on  $\Delta_{i,t}$  through the covariance of  $\mathbf{v}_{i,t}^{G} \sim \mathcal{N}(0, \Delta_{i,t}^{2}/12)$ . Therefore, the rate  $R_{i}$  allocated to sensor i can be tuned by adjusting the quantizer step size  $\Delta_{i,t}$  of the ECDQ.

# D. Least MSE estimation

In Fig. 2(c), we assume that the Kalman filter block computes the least MSE estimates  $\hat{\mathbf{x}}_{t|t-1}^G = \mathbb{E}(\mathbf{x}_t|\boldsymbol{\eta}_{1:t-1}^G)$  and  $\hat{\mathbf{x}}_{t|t}^G = \mathbb{E}(\mathbf{x}_t|\boldsymbol{\eta}_{1:t}^G)$  recursively by  $\hat{\mathbf{x}}_{t|t-1}^G = A\hat{\mathbf{x}}_{t-1|t-1}^G$  and  $\hat{\mathbf{x}}_{t|t}^G = \hat{\mathbf{x}}_{t|t-1}^G + L_t \boldsymbol{\eta}_t^G$  with the initial condition  $\hat{\mathbf{x}}_{1|1} = 0$ . Here,

$$L_t = P_{t|t-1}C^{\top} (CP_{t|t-1}C^{\top} + V)^{-1}$$
 (5)

is the Kalman gain computed from the Riccati recursion

$$P_{t|t}^{-1} = P_{t|t-1}^{-1} + C^{\top} V^{-1} C$$
 (6a)

$$P_{t+1|t} = AP_{t|t}A^{\top} + FF^{\top}.$$
(6b)

Matrices  $P_{t|t} \in \mathbb{S}^n_{++}$  and  $P_{t+1|t} \in \mathbb{S}^n_{++}$  represent the corresponding estimation error covariances

$$P_{t|t} = \text{Cov}(\mathbf{x}_t - \hat{\mathbf{x}}_{t|t}^G), \ P_{t+1|t} = \text{Cov}(\mathbf{x}_{t+1} - \hat{\mathbf{x}}_{t+1|t}^G).$$

We assume that the same Kalman gains are used in Fig. 2(a) and (b) as well. Since random variables in Fig. 2(a) and (b) share the same second order statistics with random variables in Fig. 2(c), the MSE performance of the Kalman filter in Fig. 2(a) and (b) is identical to the MSE performance in Fig. 2(c). That is, we have

$$P_{t|t} = \text{Cov}(\mathbf{x}_t - \hat{\mathbf{x}}_{t|t}), \ P_{t+1|t} = \text{Cov}(\mathbf{x}_{t+1} - \hat{\mathbf{x}}_{t+1|t}).$$

for Fig. 2(a) and (b). The next lemma provides an alternative expression of  $I(\theta_{i,t}^{\rm G};\eta_{i,t}^{\rm G})$  defined above.

**Lemma 3:** If  $L_t$  in Fig. 2(c) are chosen to be the Kalman gains defined by (5), then  $I(\boldsymbol{\theta}_{i,t}^{\rm G}; \boldsymbol{\eta}_{i,t}^{\rm G}) = I(\mathbf{x}_t; \boldsymbol{\eta}_{i,t}^{\rm G} | \boldsymbol{\eta}_{1:t-1}^{\rm G}).$ 

*Proof:* Please refer to the extended version.

<sup>&</sup>lt;sup>4</sup>The extended version is available at http://sites.utexas.edu/tanaka/files/2020/09/JT\_acc2021.pdf

# E. Sensor Resource Allocation (SRA) Problem

We are now ready to state the main problem studied in this paper. For each i=1,2,...,M, let  $\alpha_i>0$  be the cost of transmitting a binary value from the sensor i to the data fusion center. We seek the best allocation of the rate  $R_i, i=1,2,...,M$  in such a way that the total communication cost  $\sum_{i=1}^{M}\alpha_iR_i$  is minimized subject to the constraint on the MSE estimation performance of the Kalman filter. Since (4) and Lemma 3 imply that  $R_i$  can be approximated by  $I(\mathbf{x}_t; \boldsymbol{\eta}_{i,t}^G | \boldsymbol{\eta}_{1:t-1}^G)$  evaluated under Fig. 2(c), in what follows, our analysis focuses on the system shown in Fig. 2(c). The SRA problem is formulated as:

$$\min \quad \frac{1}{T} \sum_{t=1}^{T} \sum_{i=1}^{M} \alpha_i I(\mathbf{x}_t; \boldsymbol{\eta}_{i,t}^{\text{G}} | \boldsymbol{\eta}_{1:t-1}^{\text{G}})$$
 (7a)

s.t. 
$$\frac{1}{T} \sum_{t=1}^{T} \mathbb{E} \|\mathbf{x}_t - \hat{\mathbf{x}}_{t|t}\|^2 \le \beta.$$
 (7b)

The decision variable is the noise covariance matrix  $V_t = \operatorname{diag}(V_{1,t},...,V_{M,t}), t=1,2,...,T.$  If  $\{V_t^*\}_{t=1}^T$  is the optimal solution to (7) and  $f^*$  is the corresponding optimal value, the argument above implies that one can construct the ECDQ-based communication system in Fig. 2(a) attaining the total network cost less than  $f^*+1.254\times\sum_{i=1}^M\alpha_i$  by selecting the quantization step sizes  $\Delta_{i,t}$  by  $\frac{\Delta_{i,t}^2}{12}=V_{i,t}^*$ . We are also interested in the infinite-horizon problem:

$$\min \quad \limsup_{T \to \infty} \frac{1}{T} \sum_{t=1}^{T} \sum_{i=1}^{M} \alpha_{i} I(\mathbf{x}_{t}; \boldsymbol{\eta}_{i,t}^{G} | \boldsymbol{\eta}_{1:t-1}^{G})$$
(8a)

s.t. 
$$\limsup_{T \to \infty} \frac{1}{T} \sum_{t=1}^{T} \mathbb{E} \|\mathbf{x}_t - \hat{\mathbf{x}}_{t|t}\|^2 \le \beta.$$
 (8b)

# III. CONVERSION TO CONVEX-CONCAVE PROGRAM

In this section, we reformulate (7) and (8) as more explicit optimization problems.

#### A. Reformulation of the SRA problem

As before, let  $P_{t|t-1}$  be the estimation error covariance of  $\mathbf{x}_t$  given  $\boldsymbol{\eta}_{1:t-1}^{\mathrm{G}}$ . Denote by  $P_{t|t-1}^{(i)}$  the estimation error covariance of  $\mathbf{x}_t$  given  $\boldsymbol{\eta}_{1:t-1}^{\mathrm{G}}$  and  $\boldsymbol{\eta}_{i,t}^{\mathrm{G}}$ . They are related by

$$P_{t|t-1}^{(i)} = (P_{t|t-1}^{-1} + C_i^{\top} V_{i,t}^{-1} C_i)^{-1}.$$

1) Mutual information: The mutual information terms in (7a) can be written as

$$I(\mathbf{x}_{t}; \boldsymbol{\eta}_{i,t}^{G} | \boldsymbol{\eta}_{1:t-1}^{G}) = h(\mathbf{x}_{t} | \boldsymbol{\eta}_{1:t-1}^{G}) - h(\mathbf{x}_{t} | \boldsymbol{\eta}_{1:t-1}^{G}, \boldsymbol{\eta}_{i,t}^{G})$$

$$= \frac{1}{2} \log \det P_{t|t-1} - \frac{1}{2} \log \det P_{t|t-1}^{(i)}$$

$$= \frac{1}{2} \log \det P_{t|t-1} + \frac{1}{2} \log \det (P_{t|t-1}^{-1} + C_{i}^{\top} V_{i,t}^{-1} C_{i})$$

$$= \frac{1}{2} \log \det (I + P_{t|t-1}^{\frac{1}{2}} C_{i}^{\top} V_{i,t}^{-1} C_{i} P_{t|t-1}^{\frac{1}{2}})$$

$$= \frac{1}{2} \log (1 + V_{i,t}^{-\frac{1}{2}} C_{i} P_{t|t-1} C_{i}^{\top} V_{i,t}^{-\frac{1}{2}})$$

$$= \frac{1}{2} \log V_{i,t}^{-1} + \frac{1}{2} \log (V_{i,t} + C_{i} P_{t|t-1} C_{i}^{\top}).$$

Introducing changes of variables  $Q_{t|t-1} := P_{t|t-1}^{-1}$ ,  $Q_{t|t} := P_{t|t}^{-1}$  and  $\delta_{i,t} := V_{i,t}^{-1}$ ,

$$\begin{split} I(\mathbf{x}_{t}; \boldsymbol{\eta}_{i,t}^{\mathrm{G}} | \boldsymbol{\eta}_{1:t-1}^{\mathrm{G}}) &= \frac{1}{2} \log \delta_{i,t} - \frac{1}{2} \log (\delta_{i,t}^{-1} + C_{i} Q_{t|t-1}^{-1} C_{i}^{\top})^{-1} \\ &= \begin{cases} \min_{\gamma_{i,t}} & \frac{1}{2} \log \delta_{i,t} - \frac{1}{2} \log \gamma_{i,t} \\ \mathrm{s.t.} & \gamma_{i,t} \leq (\delta_{i,t}^{-1} + C_{i} Q_{t|t-1}^{-1} C_{i}^{\top})^{-1} \end{cases} \\ &= \begin{cases} \min_{\gamma_{i,t}} & \frac{1}{2} \log \delta_{i,t} - \frac{1}{2} \log \gamma_{i,t} \\ \mathrm{s.t.} & \begin{bmatrix} \delta_{i,t} - \gamma_{i,t} & \delta_{i,t} C_{i} \\ C_{i}^{\top} \delta_{i,t} & Q_{t|t-1} + C_{i}^{\top} \delta_{i,t} C_{i} \end{bmatrix} \succeq 0. \end{cases} \tag{9} \end{split}$$

The last equality is obtained by applying the matrix inversion lemma and the Schur complement formula to the constraint.

2) MSE: The MSE terms in (7b) can be written as

$$\mathbb{E}\|\mathbf{x}_{t} - \hat{\mathbf{x}}_{t|t}^{G}\|^{2} = \operatorname{Tr}(P_{t|t}) = \operatorname{Tr}(Q_{t|t}^{-1})$$

$$= \begin{cases} \min_{S_{t}} & \operatorname{Tr}(S_{t}) \\ \text{s.t.} & Q_{t|t}^{-1} \leq S_{t} \end{cases} = \begin{cases} \min_{S_{t}} & \operatorname{Tr}(S_{t}) \\ \text{s.t.} & \begin{bmatrix} S_{t} & I \\ I & Q_{t|t} \end{bmatrix} \succeq 0. \end{cases}$$

$$(10)$$

3) Reformulation of (7): From (9), (10) and (6), the SRA problem (7) can be written as

min 
$$\frac{1}{T} \sum_{t=1}^{T} \sum_{i=1}^{M} \frac{\alpha_i}{2} (\log \delta_{i,t} - \log \gamma_{i,t})$$
 (11a)

s.t. 
$$\begin{bmatrix} \delta_{i,t} - \gamma_{i,t} & \delta_{i,t} C_i \\ C_i^\top \delta_{i,t} & Q_{t|t-1} + C_i^\top \delta_{i,t} C_i \end{bmatrix} \succeq 0, \quad (11b)$$

$$\begin{bmatrix} S_t & I \\ I & Q_{t|t} \end{bmatrix} \succeq 0, \quad \frac{1}{T} \sum\nolimits_{t=1}^{T} \mathrm{Tr}(S_t) \leq \beta, \quad \quad (11c)$$

$$Q_{t|t} = Q_{t|t-1} + \sum_{i=1}^{M} \delta_{i,t} C_i^{\top} C_i,$$
 (11d)

$$Q_{t|t-1}^{-1} = AQ_{t-1|t-1}^{-1}A^{\top} + FF^{\top}.$$
 (11e)

with decision variables  $(\delta_{i,t},\gamma_{i,t})$  for i=1,...,M and t=1,...,T,  $S_t$  for t=1,...,T and  $(Q_{t|t},Q_{t|t-1})$  for t=2,...,T. The constraints (11b) and (11c) are imposed for t=1,2,...,T while the constraints (11d) and (11e) are imposed for t=2,...,T with the boundary constraint  $Q_{1|1}=P_{1|1}^{-1}$ . Notice that (11b)-(11d) are convex constraints on the decision variables, while the last constraint (11e) is not. In the next proposition, we claim that (11e) can be replaced by a convex constraint without changing the nature of the problem. More precisely, introduce a new problem:

$$\min \quad \frac{1}{T} \sum_{t=1}^{T} \sum_{i=1}^{M} \frac{\alpha_i}{2} (\log \delta_{i,t} - \log \gamma_{i,t})$$
 (12a)

s.t. 
$$\begin{bmatrix} \delta_{i,t} - \gamma_{i,t} & \delta_{i,t} C_i \\ C_i^\top \delta_{i,t} & Q_{t|t-1} + C_i^\top \delta_{i,t} C_i \end{bmatrix} \succeq 0, \quad (12b)$$

$$\begin{bmatrix} S_t & I \\ I & Q_{t|t} \end{bmatrix} \succeq 0, \quad \frac{1}{T} \sum_{t=1}^{T} \text{Tr}(S_t) \le \beta, \quad (12c)$$

$$Q_{t|t} = Q_{t|t-1} + \sum_{i=1}^{M} \delta_{i,t} C_i^{\top} C_i,$$
 (12d)

$$Q_{t|t-1}^{-1} \succeq AQ_{t-1|t-1}^{-1}A^{\top} + FF^{\top}$$
 (12e)

which is different from (11) only in that the equality constraint (11e) is replaced by the inequality constraint (12e).

**Proposition 1:** Let  $J_1^*$  and  $J_2^*$  be the optimal values of (11) and (12), respectively. Then,  $J_1^* = J_2^*$ . Moreover, if  $(\delta^*_{i,t},\gamma^*_{i,t},S^*_t,Q^*_{t|t},Q^*_{t|t-1})$  is an optimal solution to (12), then an optimal solution to (11) is given by  $(\delta_{i,t}^*,\gamma_{i,t}^*,S_t^*,Q_{t|t}^{**},Q_{t|t-1}^{**})$  where  $Q_{t|t}^{**}$  and  $Q_{t|t-1}^{**}$  are recursively defined by

$$Q_{t|t-1}^{**-1} = AQ_{t-1|t-1}^{**-1}A^{\top} + FF^{\top}$$
 (13a)

$$Q_{t|t}^{**} = Q_{t|t-1}^{**} + \sum_{i=1}^{M} \delta_{i,t}^{*} C_{i}^{\top} C_{i}$$
 (13b)

with  $Q_{1|1}^{**}=Q_{1|1}^{*}.$  Proof: Please refer to the extended version.

It is elementary to show that (12e) can be written as an equivalent linear matrix inequality (LMI) condition. Consequently, the SRA problem (7) can be equivalently written as

$$\min \quad \frac{1}{T} \sum_{t=1}^{T} \sum_{i=1}^{M} \frac{\alpha_i}{2} (\log \delta_{i,t} - \log \gamma_{i,t})$$
 (14a)

s.t. 
$$\begin{bmatrix} \delta_{i,t} - \gamma_{i,t} & \delta_{i,t}C_i \\ C_i^{\top} \delta_{i,t} & Q_{t|t-1} + C_i^{\top} \delta_{i,t}C_i \end{bmatrix} \succeq 0, \qquad (14b)$$
$$\begin{bmatrix} S_t & I \\ I & Q_{t|t} \end{bmatrix} \succeq 0, \quad \frac{1}{T} \sum_{t=1}^{T} \operatorname{Tr}(S_t) \leq \beta, \qquad (14c)$$

$$\begin{bmatrix} S_t & I \\ I & Q_{t|t} \end{bmatrix} \succeq 0, \quad \frac{1}{T} \sum_{t=1}^T \text{Tr}(S_t) \le \beta, \quad (14c)$$

$$Q_{t|t} = Q_{t|t-1} + \sum_{i=1}^{M} \delta_{i,t} C_i^{\top} C_i.$$
 (14d)

$$\begin{bmatrix} Q_{t|t-1} & Q_{t|t-1}A & Q_{t|t-1}F \\ A^{\top}Q_{t|t-1} & Q_{t-1|t-1} & 0 \\ F^{\top}Q_{t|t-1} & 0 & I \end{bmatrix} \succeq 0. \quad (14e)$$

Note that (14) is the problem of minimizing the difference of convex functions subject to convex constraints (14b)-(14e).

Before we proceed, we remark that the infinite-horizon, time-invariant counterpart (8) of the SRA problem can also be formulated as:

$$\min \quad \sum_{i=1}^{M} \frac{\alpha_i}{2} (\log \delta_i - \log \gamma_i)$$
 (15a)

$$\text{s.t.} \quad \begin{bmatrix} \delta_i - \gamma_i & \delta_i C_i \\ C_i^\top \delta_i & \hat{Q} + C_i^\top \delta_i C_i \end{bmatrix} \succeq 0, \ \forall i = 1, ..., M, \ (15b)$$

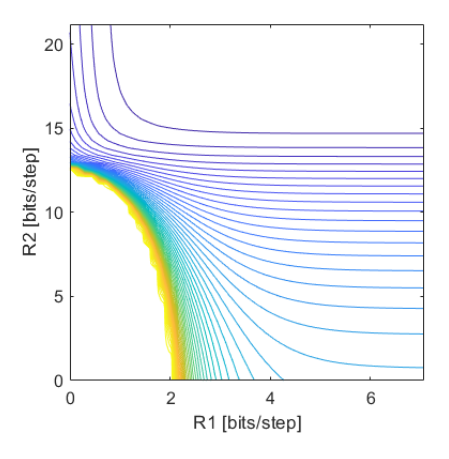
$$Q = \hat{Q} + \sum\nolimits_{i=1}^{M} \delta_{i} C_{i}^{\top} C_{i}, \ \operatorname{Tr}(S) \leq \beta, \tag{15c}$$

$$\begin{bmatrix} S & I \\ I & Q \end{bmatrix} \succeq 0, \quad \begin{bmatrix} \hat{Q} & \hat{Q}A & \hat{Q}F \\ A^{\top}\hat{Q} & Q & 0 \\ F^{\top}\hat{Q} & 0 & I \end{bmatrix} \succeq 0. \quad (15d)$$

#### B. Nonconvexity of the SRA problem

Currently, it is not known to the authors if the SRA problem can be formulated as a convex optimization problem. Since the formulation (15) is nonconvex in its variables, it may admit multiple local minima. To see that multiple and distinct local minima can indeed occur, notice that (15) can be stated as a linear function minimization problem over the feasible rate region  $\mathcal{R}_{\beta}$ :

$$\min_{(R_1,\dots,R_M)\in\mathcal{R}_\beta} \sum_{i=1}^M \alpha_i R_i \tag{16}$$



The minimum MSE error  $\beta$  achievable under various rate assignments  $(R_1, R_2)$ . Each sub-level set corresponds to the rate region  $\mathcal{R}_{\beta}$ . Clearly, they are nonconvex sets in general.

where  $\mathcal{R}_eta \in \mathbb{R}^M$  is the set of rate allocation under which (8b) (i.e., the MSE less than or equal to  $\beta$ ) is achievable:

$$\mathcal{R}_{\beta} = \{(R_1,...,R_M) \in \mathbb{R}^M : \text{There exists } Q, \hat{Q}, S \text{ and } \{\delta_i,\gamma_i\}_{i=1}^M \text{ such that } \delta_i = 2^{2R_i}\gamma_i \text{ for } i=1,...,M \text{ and } (15b)\text{-}(15d) \text{ hold.} \}$$

For each  $\beta$ , the rate region  $\mathcal{R}_{\beta}$  can be characterized by an SDP feasibility problem. Fig. 3 shows feasibility regions  $\mathcal{R}_{\beta}$ for various  $\beta$  when system parameters are set to

$$A = \begin{bmatrix} 3 & -1 \\ 1 & -1 \end{bmatrix}, \ C = \begin{bmatrix} 1 & 0 \\ 0 & 1 \end{bmatrix} \ \text{and} \ F = \begin{bmatrix} -0.5 & 0.5 \\ 0.5 & 0.5 \end{bmatrix}.$$

Fig. 3 shows an instance in which  $\mathcal{R}_{\beta}$  is a nonconvex set.

#### IV. ALGORITHMS

In this section, we propose two heuristic iterative algorithms to solve the SRA problem. Although we will focus on the infinite-horizon time-invariant case (15), the proposed approach is also applicable to the finite-horizon time-varying case (14). Despite the nonconvex nature of (15), we observe that stationary points obtained by the proposed algorithms often provide satisfactory solutions in practice.

# A. Convex-concave procedure

Since  $\log \delta_i$  is the only source of nonconvexity in (15), the class of convex-concave procedures [10] is applicable. Here, we consider the linear approximation of  $\log \delta_i$  around a nominal point  $\hat{\delta}_i$ , which provides an upper bound, i.e.,  $\log \delta_i \leq \frac{1}{\hat{\delta}_i} (\delta_i - \hat{\delta}_i) + \log \hat{\delta}_i$  and  $\hat{\delta}_i$  is the value of  $\delta_i$  obtained from the previous iteration. Consequently, for any  $\hat{\delta}_i > 0$ , the value of the following convex optimization problem with decision variables  $S, Q, \hat{Q}$  and  $\{\delta_i, \gamma_i\}_{i=1}^M$  provides an upper bound to the value of (15):

$$\min \sum_{i=1}^{M} \frac{\alpha_i}{2} (\delta_i / \hat{\delta}_i - 1 + \log \hat{\delta}_i - \log \gamma_i)$$
 (17a)

Proposed approach is summarized in Algorithm 1. Convergence of this class of algorithms is known [10].

# Algorithm 1: Convex-Concave Procedure (CCP)

```
Initialize f^{(0)} \leftarrow +\infty; \hat{\delta}_i \leftarrow 1 for i=1,2,...,M; for k=1,2,... do Solve (17); (\delta^k, \gamma^k, S^k, Q^k, \hat{Q}^k) \leftarrow \text{Optimal solution to (17)}; f^k \leftarrow \text{Optimal value of (17)}; \hat{\delta}_i \leftarrow \delta^k \text{ for } i=1,2,...,M; Break if f^{k-1}-f^k is sufficiently small;
```

# B. Alternating direction method of multipliers (ADMM)

In this subsection, we apply the ADMM [17] to (15). Notice that (15) can be expressed as the ADMM form as

min 
$$f(j) + g(z)$$
  
s.t.  $\delta = \delta', \gamma = \gamma',$ 

where  $j=\{\delta,\gamma\},\ z=\{\delta',\gamma',Q,\hat{Q},S\}$  and g is the indicator function for the convex set C characterized by (15b)-(15d). Setting  $z'=\{\delta',\gamma'\}$  and  $u=\{u_1,u_2\}$ , the augmented Lagrangian is

$$L_{\rho}(j, z, u) = f(j) + g(z) + (\rho/2) \|j - z'^{k} + u^{k}\|_{2}^{2}$$

where  $\rho$  is a penalty parameter and u is the set of Lagrangian multipliers. The ADMM iterations for this problem are

$$j^{k+1} := \underset{j}{\arg\min} \{ f(j) + (\rho/2) \| j - z'^k + u^k \|_2^2 \},$$
  

$$z^{k+1} := \Pi_c(j^{k+1} + u^k),$$
  

$$u^{k+1} := u^k + j^{k+1} - z'^{k+1}.$$

Due to the nonconvexity of f, the j-update step involves a nonconvex optimization. Therefore, in the j-update step, we replaced f(j) with its convex upper bound  $\hat{f}(\hat{\delta};j)$  by considering a linear approximation of the  $\log \delta_i$  terms around the current iterate  $\hat{\delta} = \delta^k$  in a similar fashion to (17). The projection operator  $\Pi_C$  is implemented by solving a Frobenius norm minimization problem subject to the convex constraints (15b)-(15d). Our proposed ADMM approach is presented in Algorithm 2.

# **Algorithm 2:** The Alternating Direction Method of Multiplier (ADMM)

```
Initialize f^{(0)} \leftarrow +\infty;

Set initial value of j, z, and u;

for k=1,2,... do
\begin{vmatrix} j^{k+1} \coloneqq \operatorname{argmin} \ (\hat{f}(\hat{\delta};j) + (\rho/2) \|j - z'^k + u^k\|_2^2); \\ z^{k+1} \coloneqq \Pi_c(j^{k+1} + u^k); \\ u^{k+1} \coloneqq u^k + j^{k+1} - z^{k+1}; \\ f^k \leftarrow \text{Current value of the objective function;} \\ \hat{\delta} \leftarrow \delta^{k+1}; \\ \text{Break if } f^k - f^{k+1} \text{ is sufficiently small;} \end{aligned}
```

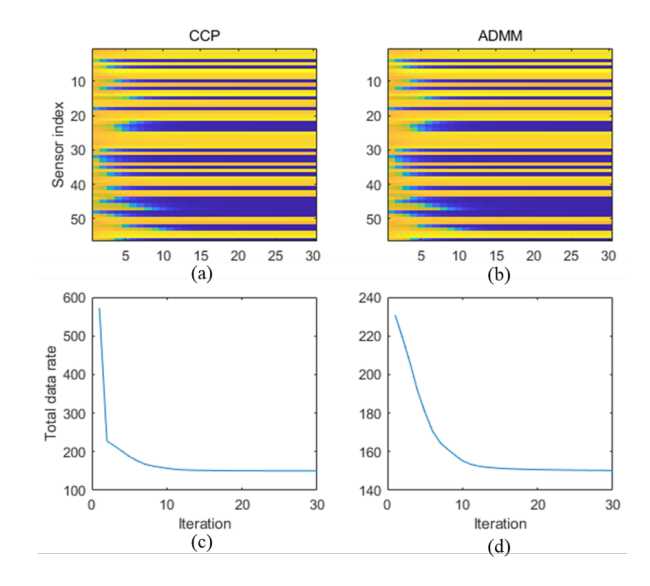


Fig. 4. CCP and ADMM data rate ( $\beta=0.1$ ). (a) Sensor data rate allocation under CCP, (b) sensor data rate allocation under ADMM, (c) total data rate under CCP, and (d) total data rate under ADMM.

#### V. NUMERICAL STUDIES

In this section, we apply Algorithms 1 and 2 to a sensor selection problem in an undamped 2D truss bridge system. The system matrix of an undamped truss bridge is calculated by via (cf. [18])  $A = M^{-1}K$  where M is mass matrix and K is stiffness matrix. A method of generating the mass matrix [19] [20] and the stiffness matrix [21] is introduced in the extended version of this paper. In this experiment, we developed a 14-node truss bridge model. Displacements and velocities of each node in both x- and y-coordinates are chosen as state variables. This results in a 56-dimensional state space, and we assume there are 56 sensors measuring individual state variables. In this study, we set  $\alpha_i = 1$  for i = 1, ..., 56. Results for the CCP and ADMM algorithms are shown in Fig. 4. In each test, the same data rate is initially allocated to each sensors, which is updated as the iteration proceeds as color-coded in Fig. 4 (a) and (b). As iteration proceeds, individual sensor's data rate changes. The total data rate is shown in Fig. 4 (c) and (d), respectively. We observe the both algorithms converge to similar solutions for individual sensor's data rate and total data rate.

Fig. 5 presents allocated data rate to each sensor after a sufficient number of CCP iterations with  $\beta=0.1,1$  and 10. We observe that the same subset of sensors is selected under  $\beta=0.1$  and 1, but the overall data rate is less under  $\beta=1$ . As  $\beta$  is increased to 10, we observe more sensors are given zero data rate. However, we also observe that the selected set of sensors is not a subset of sensors selected under  $\beta=1$ .

Fig. 6 shows the number of sensors allocated with nonzero data rate by CCP tested over a wide range of the  $\beta$  values. We observe a decrease tendency, although the relationship is not necessarily monotone. This plot exhibits a sparsity-promoting property of the proposed method, which is a reminiscent of the widely used  $\ell_1$  heuristics.

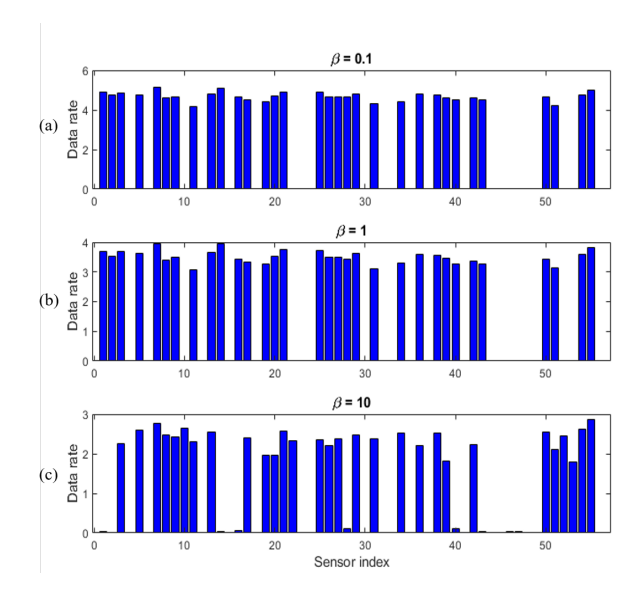


Fig. 5. Data rate allocation obtained by CCP with (a)  $\beta=0.1$  (b)  $\beta=1$  (c)  $\beta=10$ .

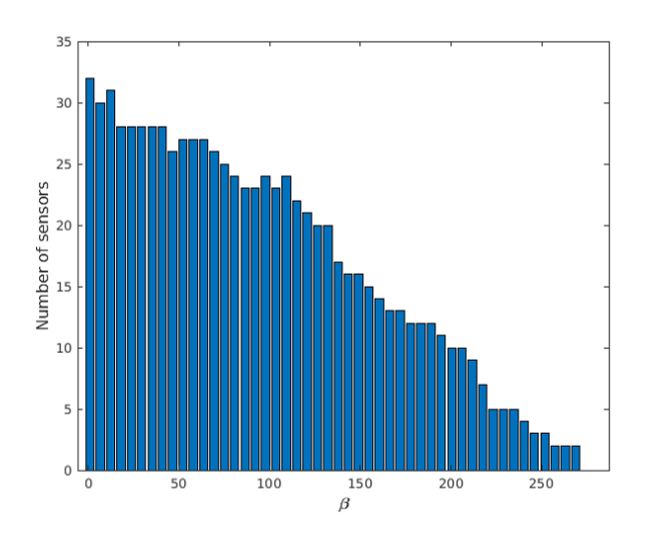


Fig. 6. Number of sensors allocated non-zero data rate by CCP tested over the range  $1 \le \beta \le 280$ .

# VI. CONCLUSION

In this paper, we considered a dynamic sensor fusion problem over a resource constrained communication network. We formulated the optimal data rate assignment problem for remote sensors as the sensor resource allocation (SRA) problem, which was shown to be reformulated as a difference-of-convex program. The convex-concave procedure (CCP) and the alternating direction method of multipliers (ADMM) were applied. The algorithms were tested on a truss bridge sensor selection problem. The sparsity-promoting property of the proposed method was numerically confirmed, indicating the effectiveness of the proposed approach as a sensor selection heuristic. Future work includes the analysis of the nonconvexity of (15) (e.g., whether local minima can be severely suboptimal), scalable implementations of CCP and ADMM, and formal analyses of the sparsity-promoting

property of the proposed method. Extension of the proposed method to finite-horizon, time-varying cases and comparison with existing approaches may be considered as future research.

#### REFERENCES

- S. Joshi and S. Boyd, "Sensor selection via convex optimization," *IEEE Transactions on Information Theory*, vol. 57, no. 2, pp. 451– 462, 2009
- [2] Y. Mo, R. Ambrosino, and B. Sinopoli, "Sensor selection strategies for state estimation in energy constrained wireless sensor networks," *Automatica*, vol. 47, no. 7, pp. 1330–1338, 2011.
- [3] G. Hovland and B. J. McCarragher, "Dynamic sensor selection for robotic systems," *Proceedings of International Conference on Robotics* and Automation, vol. 1, pp. 272–277, 1997.
- [4] D. C. Kammer, "Sensor placement for on-orbit modal identification and correlation of large space structures," *American Control Confer*ence, pp. 2984–2990, 1990.
- [5] L. Yao, W. Sethares, and D. Kammer, "Sensor placement for on-orbit modal identification of large space structure via a genetic algorithm," *IEEE International Conference on Systems Engineering*, pp. 332–335, 1992.
- [6] A. J. Walcker, "Model-based hybrid framework for live load carrying performance monitoring of bridges," 2017.
- [7] F. Xiao, J. L. Husley, G. S. Chen, and Y. Xiang, "Optimal static strain sensor placement for truss bridges," *International Journal of Distributed Sensor Networks*, vol. 13, no. 5, 2017.
- [8] F. Zhao and L. Guibas, Wireless sensor networks: An information processing approach. Morgan Kaufmann, 2004.
- [9] V. Isler and R. Bajcsy, "The sensor selection problem for bounded uncertainty sensing models," *IEEE Transactions on Automation Science* and Engineering, vol. 3, no. 4, pp. 372–381, 2006.
- [10] T. Lipp and S. Boyd, "Variations and extension of the convex–concave procedure," *Optimization and Engineering*, vol. 17, no. 2, pp. 263–287, 2016
- [11] T. M. Cover and J. A. Thomas, *Elements of information theory*. John Wiley & Sons, 2012.
- [12] S. Yüksel, "Jointly optimal LQG quantization and control policies for multi-dimensional systems," *IEEE Transactions on Automatic Control*, vol. 59, no. 6, pp. 1612–1617, 2013.
- [13] T. Tanaka, K. H. Johansson, T. Oechtering, H. Sandberg, and M. Skoglund, "Rate of prefix-free codes in LQG control systems," pp. 2399–2403, 2016.
- [14] M. S. Derpich and J. Ostergaard, "Improved upper bounds to the causal quadratic rate-distortion function for gaussian stationary sources," *IEEE Transactions on Information Theory*, vol. 58, no. 5, pp. 3131– 3152, 2012.
- [15] R. Zamir and M. Feder, "On universal quantization by randomized uniform/lattice quantizers," *IEEE Transactions on Information Theory*, vol. 38, no. 2, pp. 428–436, 1992.
- [16] E. Silva, "A unified framework for the analysis and design of networked control systems," Ph.D. dissertation, University of Newcastle, 2009.
- [17] S. Boyd, N. Parikh, E. Chu, B. Peleato, and J. Eckstein, "Distributed optimization and statistical learning via the alternating direction method of multiplierssensor selection strategies for state estimation in energy constrained wireless sensor networks," Foundations and Trends in Machine Learning, vol. 3, no. 1, pp. 1–122, 2011.
- [18] L. S. Andrés. Undamped modal analysis of mdof systems. [Online]. Available: https://rotorlab.tamu.edu/TRIBGROUP/default.htm
- [19] C. A. Felippa. (2004) Introduction to finite element methods. [Online]. Available: https://vulcanhammernet.files.wordpress.com/2017/01/ifem. pdf
- [20] R. R. Craig Jr. and A. J. Kurdila, Fundamentals of structural dynamics. John Wiley & Sons, 2006.
- [21] A. Kassimali, Matrix analysis of structures. Cengage Learning, 2012.